Detection of fibrinogen monolayers on mica by the colloid enhancement

Małgorzata Nattich-Rak, Zbigniew Adamczyk, Monika Wasilewska, Marta Radziszewska

J. Haber Institute of Catalysis and Surface Chemistry, Polish Academy of Sciences, ul. Niezapominajek 8, 30-239 Cracow, Poland
Phone: 0048 12 6395104; Fax: 0048 12 425923; E-mail: ncnattic@cyf-kr.edu.pl
Keywords: adsorption of latex on fibrinogen, colloid enhancement of protein layers, fibrinogen, fibrinogen monolayers by mica, irreversible adsorption of colloid particles

ABSTRACT

Physicochemical properties of bovine plasma fibrinogen (Fb) in electrolyte solutions were characterised, comprising the diffusion coefficient (hydrodynamic radius), electrophoretic mobility (zeta potential) and the isoelectric point, found to be at pH=5.8. Similar electrokinetic measurements were performed for the mica substrate using the streaming potential cell. The kinetics of Fb adsorption on mica under diffusion-controlled transport was also studied. The surface concentration of Fb on mica was determined directly by AFM counting. By adjusting the time of adsorption, and bulk Fb concentration, monolayers of desired coverage were produced. It was confirmed that Fb adsorbed irreversibly on mica both at pH=3.5 and pH=7.4 (physiological value). It was postulated that in the latter case, where both the substrate and fibrinogen molecules were negatively charged, adsorption was due to heterogeneous charge distribution over the protein molecule. In order to check this hypothesis, monolayers of Fb on mica were studied using the colloid enhancement (CE) method, in which negatively and positively charged latex particles were used. Results of these experiments were quantitatively interpreted in terms of the fluctuation theory assuming that adsorption sites consisted of two and three Fb molecules, for pH=3.5 and 7.4, respectively. This allowed one to determine limits of applicability of the classical DLVO theory and confirm a heterogeneous charge distribution over the Fb molecule. It was also concluded that the CE method can be used for a sensitive determination of the Fb bulk concentration for the range inaccessible for other methods, i.e., for 0.1ppm and below. Another effect of vital significance confirmed in this work was that for some range of fibrinogen coverage both the negative and positive latexes efficiently adsorbed. This indicates the formation of superadsorbing surfaces having potential significance for various filtration processes.

INTRODUCTION

Adsorption of proteins at solid/electrolyte interfaces has an essential significance because it is involved in thrombosis, artificial organ failure, plaque formation, fouling of contact lenses and heat exchangers, ultrafiltration and membrane filtration units. On the other hand, controlled protein deposition on various surfaces is a prerequisite of their efficient separation and purification by chromatography, filtration, electrophoresis, for biosensing, bioreactors, immunological assays, etc.

Because of its major significance, numerous experimental works have been devoted to quantify protein adsorption on various substrates using the solution depletion methods (Ramsden 1993), the gravimetric methods, especially the quartz microbalance (QCM) (Choi et al. 2002; Reisch et al. 2009), optical methods such as ellipsometry and reflectometry (Buijs et al. 1996, 1997; Melmsten 1994), fluorescence methods (Wertz and Santore 2001; Yoon et al. 1996) and isotope labeling (Zembala and Dejardin 1994; Zembala et al. 1998). For the low coverage range, the electron microscopy and the AFM methods can be quite efficient in a direct determination of protein coverage (Hall and Slayter 1959; Toscano and Santore 2006).

However, despite a significant progress in the field of protein adsorption, there are still discrepancies, even conflicting reports in the literature, concerning the kinetics of this process, maximum coverage, and reversibility aspects. This is mainly caused by a limited availability of direct experimental techniques working under dynamic conditions.

One of few such *in situ* methods for determining protein adsorption kinetics and properties of their monolayers is based on the streaming potential measurements (Adamczyk et al.

1999b; Hayes et al. 1999; Vasina and Dejardin 2004; Wasilewska and Adamczyk 2010; Zembala and Adamczyk 2000; Zembala et al. 2003). However, a disadvantage of such measurements is a tedious and time consuming cell assembling prior to experiments, sealing problems and the necessity of determining the correction due to surface conductance of the cell.

In this work, we propose another method of detecting protein layers on solid substrates under the wet, *in situ* conditions. The technique, refereed to as the colloid enhancement (CE), consist in unspecific deposition of larger colloid particles onto protein monolayers under well-controlled transport conditions. This enables one to determine a functional relationship between the amount of adsorbed protein (invisible agent) and the amount of adsorbed colloid, which can be assessed quantitatively via microscope counting. Knowing this function one can elaborate a protocol for an efficient determination of protein concentration in the bulk suspension, at the level of 0.1ppm and less, which is not accessible for other experimental methods.

Additionally, using the CE measurements, important clues on the structure of protein monolayers, especially charge density distribution can be gained in a simple way.

In this work we focus our attention on fibrinogen (Fb) that plays a fundamental role in blood clotting, platelet adhesion, thrombosis, angiogenesis, wound healing and tumor growth. Fibrinogen is present in blood at concentration range of 2.6 to 3mg·cm^{-3} making it the third most prevalent plasma protein. It is also one of the most relevant protein that is adsorbed on biomaterial surfaces.

MATERIAL AND METHODS

Material

Fibrinogen from bovine plasma, fraction I, type IV (65% protein, containing approximately 20% sodium chloride and 15% sodium citrate) was purchased from Sigma (F4753) and used without further purification. Protein was in 93% clottable. The purity of the Fb solution was checked by the dynamic surface tension measurements carried out using the pendant drop shape method. There was practically no change in the surface tension of the 10ppm solution of Fb within the time of two hours, which is much larger than the typical time of DLS and deposition measurements, lasting 15-30 minutes.

Ruby muscovite mica obtained from Continental Trade was used as a substrate, and was cleaved immediately prior to use without any pretreatment.

Water was purified using a Millipore Elix 5 apparatus. Chemical reagents (buffers, electrolytes) were of analytical grade, and used without further purification. Protein solutions of Fb concentration in the range of 0.5-50.0ppm were prepared as follows: the protein powder was dissolved in NaCl aqueous solution having the ionic strength of 1·10^{-3} or 1·10^{-2}M. The pH of these Fb solutions was regulated by addition of HCl or NaOH. Then, the suspension was gently mixed using a magnetic stirrer, and filtered through the Millex®-GS 0.45μm filter to eliminate aggregates and impurities. The temperature of experiments was kept constant at 293±0.1K.

Positively charged amidine polystyrene latex (Invitrogen) and negatively charged sulfonate polystyrene latex (synthesized in our laboratory) were used in this work.

Methods

The diffusion coefficient of Fb under various conditions was determined by dynamic light scattering (DLS), using the Zetasizer Nano ZS Malvern instrument (measurement range of 0.6nm to 6.0μm). The Nano ZS instrument incorporates non-invasive backscatter (NIBSTM) optics. This technique measures the time-dependent fluctuations in the intensity of scattered light which occur because particles undergo Brownian motion. Analysis of these intensity fluctuations enables the determination of the diffusion coefficients of particles which are converted into a size distribution.

The microelectrophoretic mobility of Fb was measured using the same Zetasizer Nano ZS Malvern instrument using the Laser Doppler Velocimetry (LDV) technique (measurement range of 3nm to 10μm). In this technique, a voltage was applied across a pair electrodes placed at both ends of a cell containing the particle dispersion. Charged particles are attracted to the oppositely charged electrode and their velocity is measured and expressed per unit field strength as the electrophoretic mobility μ_e. Then, the zeta potential was calculated using Henry's equation

$$\zeta = \frac{3\eta}{2\varepsilon F(\kappa a)}\,\mu_e \qquad (1)$$

where ζ is the zeta potential of proteins, η is the dynamic viscosity of water, μ_e is the electrophoretic mobility, ε is the dielectric constant of water and $F(\kappa a)$ the function of the dimensionless parameter $\kappa a = a/Le$, $Le = (\varepsilon kT / 2e^2 I)^{1/2}$ is the double-layer thickness, e the elementary charge, k the Boltzman constant, T the absolute temperature, $I = \frac{1}{2}(\Sigma_i c_i z_i^2)$ is the ionic strength, c_i the ion concentrations, z^i is the ion valency and a is the characteristic dimension of a particle or a protein particle (e.g. its hydrodynamic radius).

AFM measurements of Fb layers were carried out using the NT-MDT Solver PRO device with scanning head SMENA SFC050L. The measurements were performed in semicontact mode using silicon probe (polysilicon cantilevers with resonance frequencies 240kHz +/-10% or 140kHz +/-10%, typical curvature radius of tip was 10nm, cone angle was less then 20°). The protein solution of a desired concentration was allowed to adsorb on surface for 5–120min. and then substrate was removed, rinsed for 30 seconds using double distilled water and dried under gentle nitrogen stream.

The latex particle size as a function of ionic strength and pH was determined by laser diffractometer (Particle Size Analyzer LS 13 320 Beckman Coulter) with an accuracy of

a few percent and independently by the DLS method using the same Malvern Zetasizer Nano ZS.

Additionally, the size of deposited latex particles was determined by the AFM measurements.

The zeta potential of the latex was determined as a function of the ionic strength and pH using the ZetaPals Brookhaven and the Zetasizer Nano ZS of Malvern.

Streaming potential measurements were carried out using a home-made apparatus described in details previously (Adamczyk et al. 2006, 2007; Wasilewska and Adamczyk 2010; Zembala and Adamczyk 2000; Zembala et al. 2003).

Particle deposition experiments were performed in the diffusion cell of the dimensions 2·2·5cm, filled up with the latex suspension, having typically the number concentration of $1\text{-}2\cdot10^{10}$cm^{-3} and appropriate ionic strength and pH value. Wet mica sheets, pre-covered by Fb monolayers of desired density, were then immersed into the latex suspension. Latex particle deposition proceeded over a desired time (up to 24 hours). The true coverage of particles was determined by a direct optical microscope counting under wet conditions, as described in our previous works (Adamczyk et al. 1999a, 2010b; Zembala and Adamczyk 2000; Zembala et al. 2003). Particles were counted over 10-20 equal sized areas randomly chosen over the mica sheet. The net number of deposited particles considered was ca. 2000, which ensures a relative precision of these measurements below 2%, as determined by a variance analysis. It is worthwhile mentioning that the coverage was determined in absolute terms, i.e., $\Theta = S_g\langle N\rangle$, where $\langle N\rangle$ is the average surface concentration of particles (number of particles per unit area) and $S_g = \pi a^2$ is the cross-section of the particle (a is the particle radius). As a consequence, the coverage represents the fraction of the entire surface area occupied by particles.

However, because of multiple scattering, the optical microscope method became less accurate for coverage exceeding 0.3. In this case the AFM method (NT MDT Integra system) working in the semi contact mode was used under dry conditions to determine the surface concentration of particles and their coverage.

RESULTS AND DISCUSSION

Initially, physicochemical characteristics of Fb, latex particles and the mica substrate were determined, comprising measurements of the diffusion coefficient (hydrodynamic diameter), microelectrophoretic mobility and the electrokinetic (zeta) potential.

It was found that the diffusion coefficient of Fb was independent of its bulk concentration, assuming an average value of $2.1\cdot10^{-7}$cm^2 s^{-1} for the ionic strength range of 10^{-2}-0.15M for pH=3.5 and 7.4. Using this value of the diffusion coefficient, the Stokes hydrodynamic radius of Fb was calculated using the known dependence (Wasilewska et al. 2009)

$$R_H = \frac{kT}{6\pi\eta D} \tag{2}$$

where: R_H is the hydrodynamic radius, D – the diffusion coefficient. It was calculated from Eq. (2), that R_H =12.1nm (see Table 1). It is interesting to observe that this is much higher than the radius of the equivalent sphere equal to 4.5nm (Wasilewska et al. 2009). This reflects an elongated shape of Fb determined from crystallographic data (see Table 1).

Table 1. Physicochemical characteristics of mica, latex particles and fibrinogen.

Property	Substance	Mica	Latex A 800	Latex L 800	Fibrinogen
Zeta potential	10^{-3}M	-63	77	-82	28
ζ [mV] pH=3.5	10^{-2}M	-52	95	-102	22
Zeta potential	10^{-3}M	-112	75	-80	-21
ζ [mV] pH=7.4	10^{-2}M	-80	95	-105	-19
R_H [nm] $I = 10^{-2}$-10^{-3}M		-	405	400	12.1
Fibrinogen, Molecular weight (340 kD)					
Molecular shape					

The electrophoretic mobility of fibrinogen as a function of pH and the ionic strength was also determined according to the method above described. Knowing the electrophoretic mobility of a particle, one can calculate the averaged number of uncompensated (free) charges per molecule N_c from the Lorenz-Stokes relationship (Wasilewska et al. 2009) and the zeta potential of fibrinogen ζ_f from Eq. (1). The latter parameter is of a primary importance for predicting the stability of fibrinogen suspensions. It was determined in this way that ζ_f was positive, equal to 22 and 28mV for pH=3.5 and the ionic strength of 10^{-2} and 10^{-3}M, respectively (Table 1). On the other hand, it was determined that for pH=7.4 ζ_f became negative, equal to -19 and -21mV for the ionic strength of 10^{-2} and 10^{-3}M, respectively (Table 1). From the electrophoretic mobility measurements, it was also found that the isoelectric point of fibrinogen (zero value of its zeta potential) was at pH=5.8.

In an analogous way, the hydrodynamic radius and microelectrophoretic mobility of latexes used in our studies were characterized. The average hydrodynamic radius of the A800 (positive) latex for the pH range 3.0-7.4 was 405nm (ionic strength 10^{-3}-10^{-2}M) and for the L800 (negative) latex it was 400nm, for the same range of pH and ionic strength. Because latex particles were spherical, which was checked by electron microscopy measurements, the geometrical diameter $2a$ was 810nm for the A800 latex and 800nm for the L800 latex.

The zeta potential of both latex samples was also determined as a function of pH and ionic strength. As can be noticed (Table 1), the A800 zeta potential was fairly independent of pH, assuming 77mV for $I=10^{-3}$M and 95mV for $I=10^{-2}$M. The zeta potential of the L800 latex was also practically independent of pH assuming an average value of –81mV (for $I=10^{-3}$M) and –104mV for $I=10^{-2}$M.

On the other hand, the zeta potential of the mica substrate was determined via the streaming potential measurements according to the procedure described in previous works (Adamczyk et al. 2010b, c; Wasilewska and Adamczyk 2010). For the ionic strength of 10^{-3}M, the zeta potential of mica was -63mV for pH=3.5 and -112mV at pH=7.4. For the ionic strength of 10^{-2}M, the zeta potential of mica was less negative, equal to -52mV for pH=3.5 and –80mV (Table 1).

These physicochemical measurements suggest that Fb should adsorb on mica for the pH=3.5 due to attractive electrostatic interactions, because the zeta potential of Fb is positive and the zeta potential of mica strongly negative (Table 1). For pH=7.4, both the Fb and mica zeta potentials were negative that is expected to prevent adsorption because of the electrostatic repulsion. In order to verify this hypothesis, systematic Fb adsorption experiments were conducted under the diffusion-controlled transport.

The number of adsorbed Fb molecules on the mica substrate immersed in the Fb suspension was determined by direct AFM counting. The topology of fibrinogen monolayers on mica determined in this way is shown in Figure 1 for $N=47$

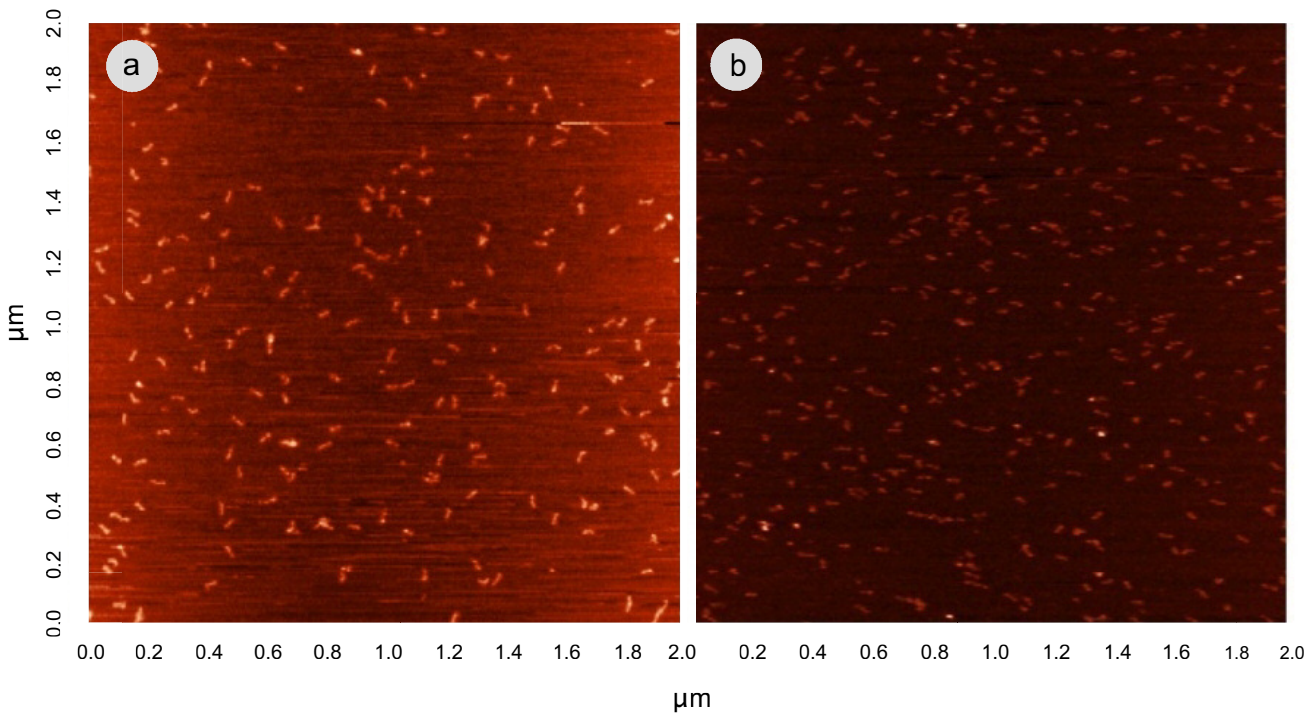

Figure 1. The topology of fibrinogen monolayers on mica determined by AFM, for pH=3.5, T=293K, $I=10^{-3}$M and the surface concentration of N equal to Part "a" 47 and part "b" 125 [μm^{-2}], respectively.

and 125μm^{-2}. Using this counting procedure the kinetics of Fb adsorption was also determined, i.e., the dependence of the reduced surface concentration of Fb N/c_b on the square root of the adsorption time $t^{1/2}$ where c_b is the bulk conctration of fibrinogen. Results of these measurements performed for $I=10^{-3}$M, pH=3.5 and $T=293$K are shown in Figure 2. As can be seen, the Fb surface concentration increased linearly with the square root of time in accordance with theoretical results, described by the following dependence (Adamczyk 2006; Adamczyk et al. 2007)

$$N = 2\left(\frac{Dt}{\pi}\right)^{1/2} n_b \tag{3}$$

where $n_b=c_b\, Av\cdot 10^{-6}/M_w$ is the number concentration of Fb molecules in the bulk, Av is the Avogadro constant).

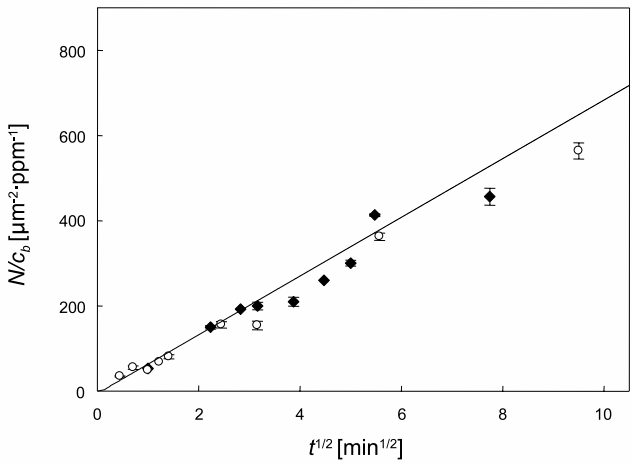

Figure 2. The dependence of the normalized surface concentration of Fb N/c_b [μm^{-2}ppm^{-1}] on the square root of the adsorption time $t^{1/2}$ [min$^{1/2}$]. The points denote the experimental results obtained for pH=3.5 and pH=7.4, $T=293$K, $I=10^{-3}$M using the AFM topological measurements and the solid line shows the theoretical results calculated from the generalized diffusion model (Adamczyk et al. 2010a).

The good agreement of experimental results with theoretical predictions, derived from Eq. (3) indicates that Fb adsorption on mica for pH=3.5 was irreversible and bulk transport controlled with negligible surface transport resistance. This seems quite obvious considering the strong attraction between Fb molecules and oppositely charged mica substrate.

Quite unexpectedly, however, an identical kinetics was also observed in the case of pH=7.4 (Figure 2), where a strong electrostatic repulsion was expected due to like sign of zeta potential of Fb and mica. As discussed in Wasilewska and Adamczyk (2010) this anomalous behaviour can be explained in terms of a heterogeneous charge distribution over the Fb molecule. Hence, besides negatively charged, the Fb molecule exhibits positively charged patches, which can form stable electrostatic bonds with mica surface. Additionally, the van der Waals attractive interaction played a role, promoting irreversible adsorption of Fb at pH=7.4.

This is an interesting finding because using Eq. (3) one can determine in a direct way the bulk concentration of the protein if it is an unknown parameter. This can be done by plotting N determined by AFM vs. the square root of adsorption time, $t^{1/2}$. Knowing the slope of this dependence sf and considering that the diffusion coefficient of Fb equals $2.1\cdot 10^{-7}$cm^2 s^{-1} ($T=293$K) one can determine the unknown concentration of fibrinogen in the bulk (in ppm) from the simple relationship

$$c_b = \frac{M_w}{A_v}\times 10^{13}\left(\frac{\pi}{2.4D}\right)^{1/2} s_f \tag{4}$$

where c_b is expressed in ppm and $s_f=\Delta N/\Delta t^{1/2}$ is expressed in μm^{-2} min$^{-1/2}$.

Using the value of the diffusion coefficient and molecular weight pertinent to fibrinogen one can express Eq. (4) in the simpler form

$$c_b = 0.014\, s_f \tag{5}$$

From Eq. (5) one can determine in a direct way the bulk concentration of Fb even below 0.1ppm, which is rather difficult using other methods.

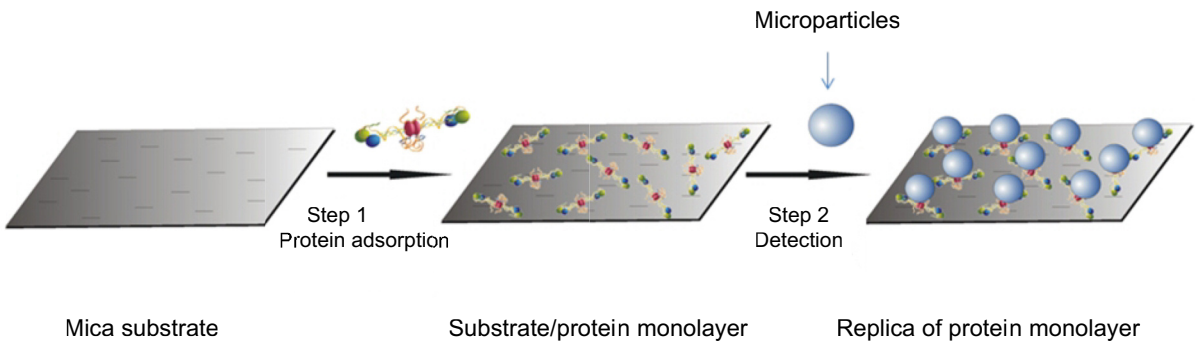

Figure 3. A schematic representation of the colloid enhancement of protein layers.

However, the AFM counting procedure, although precise, is rather tedious to perform, requiring sophisticated apparatus. Therefore, in our work we have studied the possibility of using a more convenient determination of fibrinogen bulk concentration based on the colloid enhancement (CE) method. The essence of this method consists in making a replica of the protein monolayer formed initially by immersion in colloid suspension in the second stage (Figure 3). The advantage of this approach is that one does not need to measure the surface concentration of Fb molecules using the AFM but merely, the surface concentration of colloid particles using the ordinary optical microscope, which is much simpler. Another advantage of the CE method is that it can be used for determining not only of the Fb monolayer density but also the charge distribution. This can enable one to explain the mechanism of the anomalous adsorption of negatively charged protein molecules on negatively charged substrates.

In order to analyse the CE results in a quantitative manner, reference kinetic data are needed for colloid particles adsorption on the bare mica surface. These kinetic studies were performed under diffusion-controlled conditions using the positively charged A800 latex, which adsorbed in an irreversible way on mica at pH range 3.5–7.4. The number of latex particles adsorbed as a function of the immersion time was determined by direct optical counting. In order to increase the reliability of these measurements additional AFM enumeration of adsorbed latex particles was performed.

The topology of the latex monolayer on mica determined by optical microscopy for Θ_L =0.1 and 0.4 is shown in Figure 4 (the latex coverage was calculated as $\Theta_L = \pi a^2 N_L$, where N_L is the latex surface concentration). Using this procedure, the kinetics of latex adsorption was determined for various ionic strength, bulk suspension concentration and pH. Examples of kinetic curves obtained for the A800 latex under diffusion-controlled transport for pH=3.5, $I=10^{-2}$ and 10^{-3}M, $n_b=1.77\cdot10^{10}$cm^{-3} are shown in Figure 5. As can be observed, the dependence of the latex coverage on the square root of the deposition time $t^{1/2}$ remains linear for $\Theta_L < 0.3$, which is in accordance with Eq. (3). This means that latex adsorption for this coverage range was controlled by the bulk transport, rather than surface blocking effects. However, for higher latex coverage, significant deviations from linearity occurred, and the kinetic curve approached gradually the limiting values Θ_{mx} =0.46 for $I=10^{-3}$ and 0.52 for 10^{-2}M (note a good agreement between the optical microscopy and AFM data). The deviations from linearity appeared because of surface blocking effects, as analysed in Adamczyk (2000, 2006), Adamczyk et al. (1999a) and Schaaf and Talbot (1989), where a theoretical model was developed based on the random sequential adsorption (RSA) approach. This allowed one to formulate the governing diffusion equations for describing latex adsorption for arbitrary ionic strength and bulk concentration (Adamczyk 2000, 2006). As can be observed in Figure 5, theoretical results obtained by numerically solving this bulk transport equation using the implicit, finite-difference

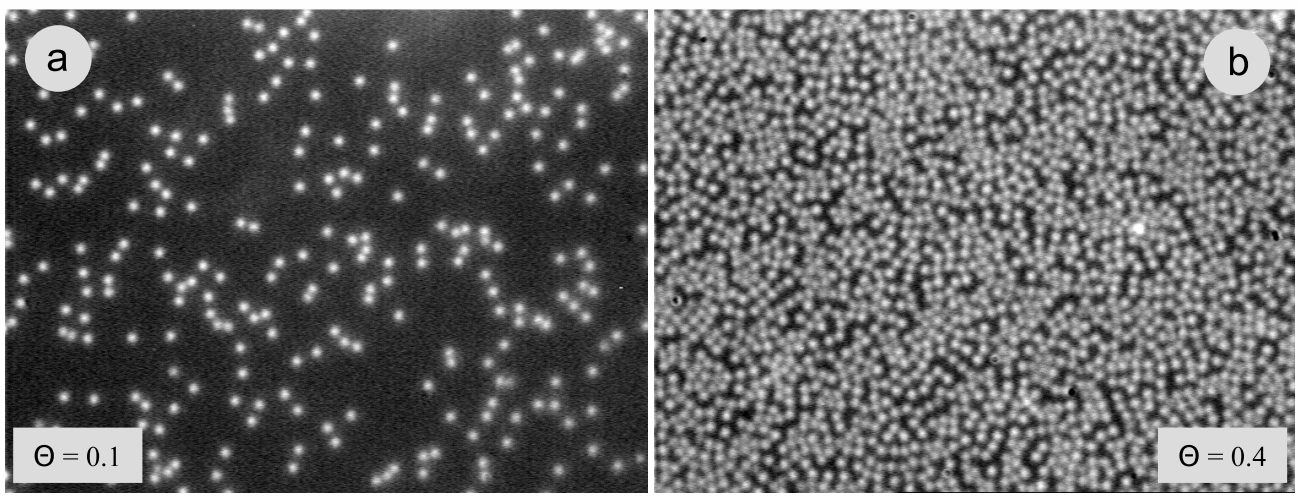

Figure 4. Monolayers of the A800 latex on mica for part "a" Θ_L=0.1, and part "b" 0.4, respectively. Optical microscopy, T=293K, $I=10^{-3}$M.

method of Crank-Nicholson (solid and dashed lines), are in an agreement with experimental data for the entire range of adsorption time and both ionic strengths.

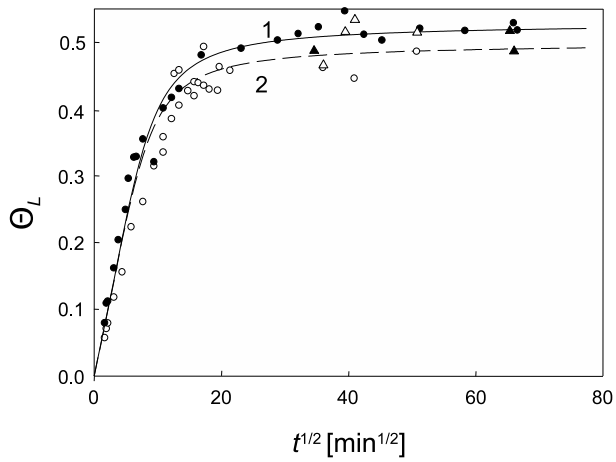

Figure 5. Deposition kinetics of the A800 latex on mica, determined by optical microscopy (full symbols) and AFM (empty symbols), for the ionic strength 10^{-3}M, T=293K, n_b=1.77·10^{10}cm^{-3}.
1. (●, ○) I=10^{-2}M,
2. (▲, △) I=10^{-3}M
The lines denote exact theoretical results calculated by solving the governing diffusion equation with the blocking effect given by the RSA model.

It should be mentioned that due to symmetry of the electrostatic interactions, the same theoretical results are predicted in the case where the latex particles exhibit a negative zeta potential and the interface a positive zeta potential, provided that the size of latex particles remains the same. Therefore, the results shown in Figure 5, obtained for homogeneous surfaces, can be used as convenient reference system for analyzing the CE results obtained for both, the positive (A800) and the negative (L800) latexes.

In the first stage of the CE experiments, a fibrinogen monolayer on mica of a desired coverage was produced. Then, the wet mica sheets were placed in the diffusion cell and latex deposition was carried out for 24 hours to attain the maximum coverage. After rinsing the mica sheets, latex was determined under in flow conditions. This procedure allowed one to avoid distortions of the Fb and latex monolayers, which is often the case when drying procedure is applied prior to microscope observations. In this way, one could determine in a reproducible way not only the latex coverage but also the homogeneity of particle distributions over the mica substrate.

The results of latex adsorption experiments expressed in terms of the normalized maximum latex coverage Θ_L / Θ_{mx} vs. the fibrinogen coverage Θ_f are shown in Figure 6 (part "a" for the negative L800 latex and in part "b" for the positive A800 latex). The conditions of these experiments were the same as for the calibration experiments involving the A800 latex sample, i.e., pH=3.5, I=10^{-3}M, n_b=1.77·10^{10}cm^{-3}. As can be seen in Figure 6a, the normalized coverage of negative latex

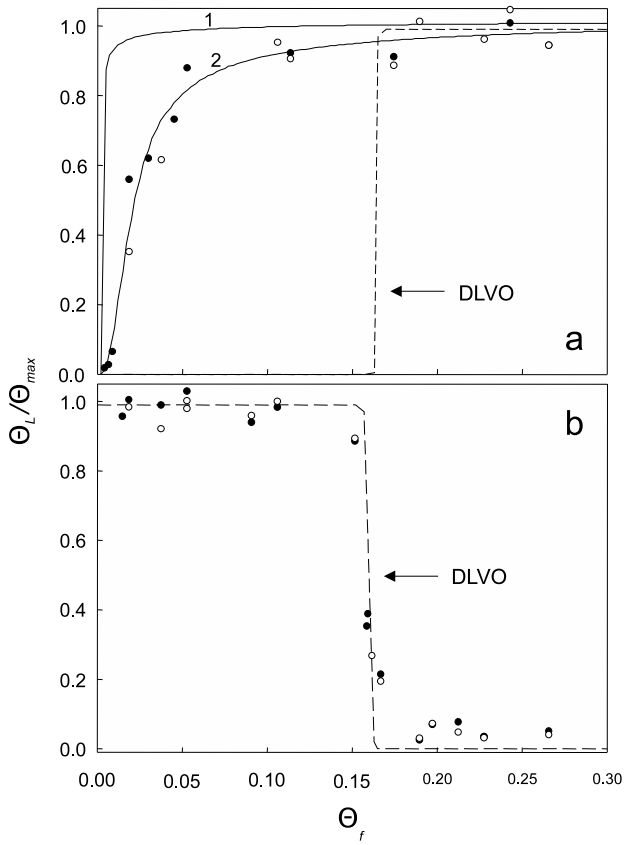

Figure 6. Part "a". The dependence of the reduced coverage of negative latex particles L800 Θ_L/Θ_{max} on the fibrinogen coverage Θ_f. The points denote the experimental results obtained by optical microscopy (●) and AFM (○), for ionic strength 10^{-3}M, pH=3.5, T=298K, n_b=1.77·10^{10}cm^{-3} deposition time 20 hours. The solid lines 1-2 denote theoretical prediction derived from Eqs. (7, 8, 10) for the adsorption site composed of one and two fibrinogen molecules, respectively. The dashed line denotes theoretical results calculated from the DLVO theory for a continuous surface charge distribution.
Part "b". The dependence of the reduced coverage of positive latex particles A800 Θ_L/Θ_{max} on the fibrinogen coverage Θ_f. The points denote the experimental results obtained by optical microscopy (●) and AFM (○), for ionic strength 10^{-3}M, pH=3.5, T=298K, n_b=1.77·10^{10}cm^{-3}. The dashed line denotes theoretical results calculated from the DLVO theory for a continuous surface charge distribution.

increased abruptly with Θ_f, attaining 0.8 for Θ_f as low as 0.05 (5%). Thus, the initial slope of the Θ_L / Θ_{mx} vs. Θ_f dependence exceeded 16, which indicates that the sensitivity of detecting Fb layers by latex deposition can be high. However, for Θ_f >0.05, the increase in the latex coverage with the Fb coverage was less steep, which prohibits an exact evaluation of Fb coverage using latex deposition data.

Qualitatively, these experimental results can be interpreted by postulating that negative latex adsorption occurred at sites formed by fibrinogen molecules on mica, bearing a positive charge at this pH.

In order to verify this hypothesis quantitatively we applied the random site model previously developed to interpret particle deposition on surfaces covered by polyelectrolytes (Adamczyk et al. 2006, 2007). The basic parameter of this approach, characterizing the density of adsorption sites (fibrinogen molecules), is defined as

$$\alpha = \pi a^2 N_s = \frac{\pi a^2}{S_g}\Theta_s = \lambda^2 \Theta_s \tag{6}$$

where N_s is the surface concentration of adsorption sites, S_g is the characteristic cross-section area of one site and

$$\lambda = \left(\frac{\pi a^2}{S_g}\right)^{1/2}$$

Assuming that in our case the sites are formed by single Fb molecules having the cross-section area $S_{gf} = 1.28 \cdot 10^{-12}\text{cm}^2$ (Adamczyk et al. 2010a, b; Wasilewska and Adamczyk 2010) and considering that $S_{gl} = \pi a^2 = 5.03 \cdot 10^{-9}\text{cm}^2$ one obtains $\lambda^2 = 3.93 \cdot 10^3$.

Knowing the α parameter one can calculate the maximum coverage of latex particles on a heterogeneous surface covered by sites from the analytical dependence (Adamczyk 2006; Adamczyk et al. 2010b; Jin et al. 1993) modified in our work to account for the fact that Θ_{mx} is a variable, rather than a constant.

$$\Theta_L = \Theta_{max}\left(1 - \frac{1 + 0.314\alpha^2 + 0.45\alpha^3}{1 + \frac{1}{\Theta_{mx}}\alpha + 0.66\alpha^3 + \alpha^{7/2}}\right) \tag{7}$$

In the limit of low coverage of sites, where $\alpha << 1$, Eq. (7) simplifies to

$$\Theta_L = \lambda^2 \Theta_s \tag{8}$$

Thus, in this case, the latex coverage should increase linearly with the site coverage.

As can be seen in Figure 6a, the theoretical results derived from Eqs. (7, 8) (curve 1) do not reflect properly the experimental data, since they predict a much steeper increase of Θ_L/Θ_{max} with the Fb coverage than experimentally observed. This indicates that adsorption of latex particles on sites consisting of single Fb molecule was not possible due to too low attractive interaction energy. An analogous phenomenon was previously observed in the case of poly(allylamine) hydrochloride and poly(ethylene imine) polyelectrolytes (Adamczyk et al. 2006, 2007), where latex particle deposition occurred at adsorption centers composed of two or more closely spaced polyelectrolyte chains.

It was shown in these works, assuming the Poisson statistics, that the coverage of adsorption sites composed of n_s or more particles is given by the expression (Adamczyk et al. 2006, 2007)

$$\Theta_s(n_s) = e^{-\bar{S}\Theta_f} \sum_{n=n_s}^{\infty} \frac{(\bar{S}\Theta_f)^n}{n!} = \frac{(\bar{S}\Theta_f)^{n_s}}{n_s!} \tag{9}$$

where $S = S^*/S_g$ and S^* is the effective interaction area, whose size is comparable with the cross-section area of the site, thus $S^* \approx 1$.

From Eq. (9) one can deduce that the coverage of sites composed of two or more Fb molecules is given by.

$$\Theta_s(2) = \frac{1}{2}\Theta_f^2$$

Considering this, one obtains from Eq. (8) following the expression for Θ_L.

$$\Theta_L = \frac{1}{2}\lambda^2 \Theta_f^2 \tag{10}$$

Thus, in this case, a parabolic dependence of Θ_L on the Fb coverage is predicted for not too high Fb coverage. This means that the number of sites composed of two Fb molecules remains low for Fb coverage not exceeding 0.1.

Substituting Eq. (10) into Eq. (7) one can calculate the maximum coverage of latex as a function of the fibrinogen coverage. As can be seen in Figure 6a, such theoretical results are in a good agreement with experimental data for the entire range of Fb coverage. In particular, the parabolic dependence, described by Eq. (10) for low Θ_f coverage is confirmed. This suggests that the CE experiments of latex deposition on fibrinogen monolayers can be exploited for an efficient determination of the bulk concentration of the protein. This can be done by rearranging Eq. (10), using Eq. (3) to express fibrinogen coverage, to the form

$$\Theta_L = \frac{1}{\pi}\lambda^2 D n_b^2 t \tag{11}$$

As can be noticed the latex coverage Θ_L is a linear function of the fibrinogen bulk concentration and the adsorption time t.

It should be remembered, however, that Eq. (11) remains valid for $\Theta_L < 0.2$.

From Eq. (11) one can deduce that knowing the slope s'_f of the Θ_L on t dependence determined experimentally, one can calculate the unknown concentration of fibrinogen in the suspension from the relationship

$$c_b = \frac{M_w}{A_v} \times 10^5 \left(\frac{\pi}{1.2\, S_{gl} S_{gf} D}\right)^{1/2} s_f'^{\,1/2} \tag{12}$$

where c_b is expressed in ppm and $s'_f = \Delta\Theta_L/\Delta t$ is expressed in min^{-1}.

Using the experimental data known for fibrinogen, one can simplify Eq. (12) to the form

$$c_b = 2.48\, s_f^{\prime\,1/2} \tag{13}$$

In this way, one can determine, using the simple optical microscopy method, the bulk concentration of Fb, for the range well below 0.1 ppm.

However, as above mentioned, Eqs. (12, 13) remain accurate for low latex coverage only. For arbitrary latex coverage range one can use Eq. (7) to calculate the unknown fibrinogen concentration, which requires a numerical solution of this nonlinear equation, however.

Except for this practical aspect, the results shown in Figure 6a have a significance for basic colloid science because they demonstrate a major role of the local charge fluctuations, induced by protein adsorption on solid substrates. This is evident, because results calculated from the classical DLVO (Derjaguin, Landau, Vervey, Overbeek) theory, shown by the dashed line in Figure 6a, deviate completely from the experimental results. The DLVO theoretical predictions were calculated by assuming a continuous, rather than a discrete, charge distribution over mica surface and by neglecting all charge fluctuations. As a consequence, the mica surface was characterized by an average value of the zeta potential, determined experimentally using the streaming potential method (Wasilewska and Adamczyk 2010). It was found that this averaged potential of the mica substrate was negative for fibrinogen coverage below 0.16, hence no deposition of negative latex could be expected, according to the DLVO theory. In reality, as can be seen in Figure 6a, a significant deposition of the negative latex was observed for $\Theta_f < 0.16$ due to local fluctuations in the charge density.

However, the DLVO theory works well for $\Theta_f > 0.16$, predicting results, which are similar to the charge fluctuation theory (see Figure 6a). This is so, because for the high coverage range, fluctuations in the Fb molecule density (local charge) within the area of interaction with the latex particles (whose cross-section area is $\lambda^2 = 3.8 \cdot 10^3$ times larger than the fibrinogen molecule cross-section area) become negligible. As a result, the local zeta potential of Fb covered mica remains close to the averaged zeta potential. This effect is further confirmed by results shown in Figure 6b, where the coverage of the positive (A800) latex is plotted against the fibrinogen coverage. As can be seen, for $\Theta_f < 0.16$, where the average zeta potential of mica remained positive, there was no latex adsorption and for $\Theta_f > 0.16$, a full adsorption of the positive A800 latex was observed. These experimental results were quantitatively accounted for by predictions stemming from the DLVO theory (see the dashed line in Figure 6a), which confirmed that local charge density fluctuations were negligible for such a high fibrinogen coverage. This observation can be exploited for a simple and accurate determination of the isoelectric point of heterogeneous surfaces covered by proteins, which is rather tedious by electrokinetic methods.

By comparing results shown in Figures 6a and 6b one can notice that they are complementary because for $\Theta_f > 0.16$ the negative latex adsorbs fully on the fibrinogen layers, whereas the positive latex does not practically adsorb. This phenomenon can be used for a simple and convenient detection of fibrinogen layers on mica, and, therefore, fibrinogen concentration in the bulk.

Another unexpected conclusion which can be drawn from these results is that for a definite range of fibrinogen coverage ($0.02 < \Theta_f < 0.16$) both the negative and positive latexes will adsorb on surfaces covered by Fb, with a comparable efficiency. Hence, such surfaces can be named superadsorbing surfaces (SAS), because they are able to remove both positive and negatively colloid particles from their suspensions. This could be of vital significance for various water filtration processes.

Analogous deposition experiments were performed for the physiological pH=7.4. As mentioned, at this pH the Fb molecules were on average negatively charged, similarly the mica substrate (Table 1). Quite unexpectedly, also in this case, the negative latex adsorbed quite efficiently for $\Theta_f > 0.05$ (see Figure 7a). These results unequivocally proved that the charge distribution over Fb molecules at this pH was highly heterogeneous. This was suggested in the recent work on the electrokinetics of fibrinogen layers on mica (Wasilewska and Adamczyk 2010). Because of the charge heterogeneity, there existed patches of positive charge on mica, formed by a few closely spaced Fb molecules, despite the fact that the average charge (zeta potential) of the interface was negative. This hypothesis seems confirmed by a good agreement of experimental results shown in Figure 7a with theoretical results stemming from the fluctuation theory, described by Eq. (7). However, in this case, the experimental results were well fitted assuming that the adsorption sites are formed by three Fb molecules.

Accordingly, the surface coverage of such sites $\Theta_s(3) = \frac{1}{6}\Theta_f^3$ and

$$\Theta_L = \frac{1}{6}\lambda^2 \Theta_f^3 \tag{14}$$

Thus, in this case the latex coverage Θ_L is expected to increase proportionally to the third power of the Fb coverage for the low coverage range.

By substituting the dependence Eq. (14) into Eq. (7) one obtains a nonlinear relationship, which well reflects the experimental results shown in Figure 7a. This suggests, as previously mentioned that Eq. (14), upon a numerical inversion procedure, can be used to calculate the unknown fibrinogen concentration in the bulk.

Formation of sites composed of three Fb molecules is understandable because the partial positive charge on fibrinogen at pH=7.4 is much smaller than it was the case for pH=3.5 (Wasilewska and Adamczyk 2010).

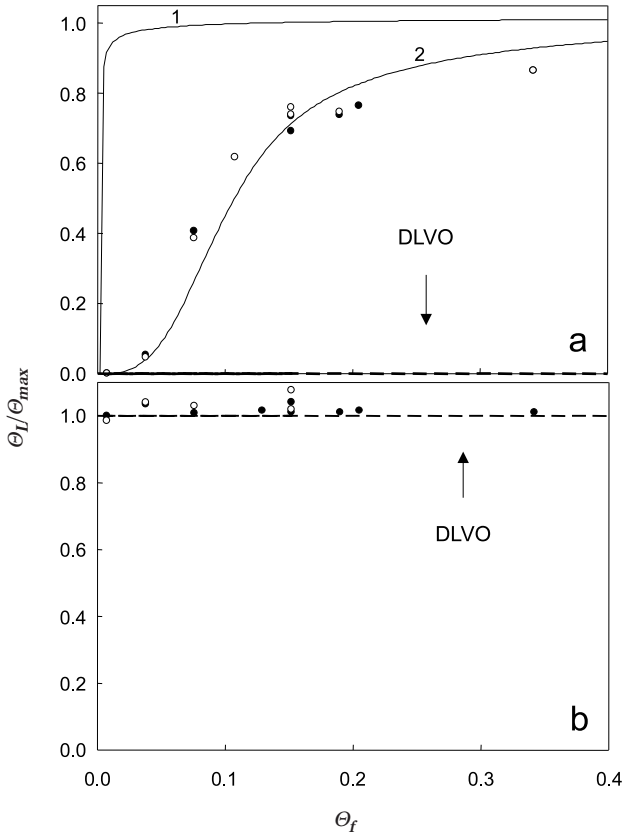

Figure 7. Part "a". The dependence of the reduced coverage of negative latex particles L800 Θ_I/Θ_{max} on the fibrinogen coverage Θ_f. The points denote the experimental results obtained by optical microscopy (●) and AFM (○), for ionic strength 10^{-2}M, pH=7.4, T=293K, $n_b=1.77\cdot10^{10}$cm^{-3} deposition time 20 hours. The solid lines 1-2 denote theoretical prediction derived from Eqs. (7, 14) for the adsorption site composed of one and three fibrinogen molecules, respectively. The dashed line denotes theoretical results calculated from the DLVO theory for a continuous surface charge distribution.
Part "b". The dependence of the reduced coverage of positive latex particles A800 Θ_I/Θ_{max} on the fibrinogen coverage Θ_f. The points denote the experimental results obtained by optical microscopy (●) and AFM (○), for ionic strength 10^{-2}M, pH=7.4, T=298K, $n_b=1.77\cdot10^{10}$cm^{-3}. The dashed line denotes theoretical results calculated from the DLVO theory for a continuous surface charge distribution.

It is interesting to note that the DLVO theory completely fails in the case of pH=7.4, because no negative latex adsorption is predicted for the entire range of (see the dashed line in Figure 7a). This is so, because as shown in Wasilewska and Adamczyk (2010) the average zeta potential of mica remains negative for $0<\Theta_f<0.4$. For the same reason, experimental results concerning the positive latex adsorption were fully accounted for by the DLVO theory (see the dashed line in Figure 7b). Hence, it was confirmed again that mica covered by fibrinogen layers of controlled coverage ($\Theta_f>0.1$), being on average negatively charged, behaves as a superadsorbing surface.

It can also be concluded that the CE experiments described above can be exploited not only for precise detection of Fb monolayers on mica but also for determination of adsorption site configuration, which is a rather unique possibility.

CONCLUDING REMARKS

It was confirmed by direct AFM measurements that fibrinogen was adsorbing irreversibly on mica surface both at pH=3.5 and pH=7.4. It was postulated that in the latter case, where the substrate and fibrinogen molecules were both negatively charged, adsorption was due to heterogeneous charge distribution over the protein molecule.

Because Fb adsorption was governed in both cases by the bulk diffusion, a sensitive method of determining the bulk concentration of the protein was proposed, based on the AFM determination of its surface concentration as a function of adsorption time.

The presence of Fb monolayers on mica was also quantitatively analysed using the colloid enhancement method. Results of these experiments were quantitatively interpreted in terms of the fluctuation theory by assuming that adsorption sites consisted of two and three Fb molecules, for pH=3.5 and 7.4, respectively. This allowed one to determine limits of the applicability of the DLVO theory and confirm the heterogeneous charge distribution over the Fb molecule. It was also demonstrated that the CE method can be used for a sensitive determination of the Fb concentration in the bulk for the range inaccessible for other methods, i.e. for 0.1ppm and below.

Another unexpected effect of vital significance for basic colloid science confirmed in this work is that for a definite range of fibrinogen coverage (depending on the pH) both the negative and positive colloid particles adsorb on surfaces covered by Fb. Superadsorbing surfaces, formed in this way can be of significance for various filtration processes.

ACKNOWLEDGEMENTS

This work was supported by the COST Action D43 Special Grant and POIG01.01.02-12-028/09-01.

REFERENCES

Adamczyk, Z. 2000. Kinetics of diffusion-controlled adsorption of colloid particles and proteins. Journal of Colloid and Interface Science 220: 477-489.
Adamczyk, Z. 2006. Particles at Interfaces: Interactions, Deposition, Structure. Academic Press, Elsevier.
Adamczyk, Z., J. Barbasz, M. Cieśla. 2010a. Kinetics of fibrinogen adsorption on hydrophilic substrates. Langmuir 26: 11934–11945.

Adamczyk, Z., A. Michna, M. Szaraniec, A. Bratek, J. Barbasz. 2007. Characterization of poly(ethylene imine) layers on mica by the streaming potential and particle deposition methods. Journal of Colloid and Interface Science 313: 86-96.

Adamczyk, Z., M. Nattich, M. Wasilewska. 2010b. Irreversible adsorption of latex particles on fibrinogen covered mica. Adsorption 16: 259-269.

Adamczyk, Z., B. Senger, J.C. Voegel, P. Schaaf. 1999a. Irreversible adsorption/deposition kinetics: A generalized approach. Journal of Chemical Physics 110: 3118-3128.

Adamczyk, Z., P. Warszyński, M. Zembala. 1999b. Influence of adsorbed colloid particles on streaming potential. Bulletin of the Polish Academy of Sciences: Chemistry 47: 239-258.

Adamczyk, Z., M. Zaucha, M. Zembala. 2010c. Zeta potential of mica covered by colloid particles: A streaming potential study. Langmuir 26: 9368-9377.

Adamczyk, Z., M. Zembala, A. Michna. 2006. Polyelectrolyte adsorption layers studied by streaming potential and particle deposition. Journal of Colloid and Interface Science 303: 353-364.

Buijs, J., P.A.W. van den Berg, J.W.Th. Lichtenbelt, W. Norde, J. Lyklema. 1996. Adsorption dynamics of IgG and its $F(ab')_2$ and Fc fragments studied by reflectometry. Journal of Colloid and Interface Science 178: 594-605.

Buijs, J., D.D. White, W. Norde. 1997. The effect of adsorption on the antigen binding by IgG and its $F(ab')_2$ fragments. Colloids and Surfaces B Biointerfaces 8: 239-249.

Choi, K.H., J.M. Friedt, F. Frederix, A. Campitelli, G. Borghs. 2002. Simultaneous atomic force microscope and quartz crystal microbalance measurements: Investigation of human plasma fibrinogen adsorption. Applied Physics Letters 81: 1335-1337.

Hall, C.E., H.S.J. Slayter. 1959. The fibrinogen molecule: its size, shape, and mode of polymerization. The Journal of Biophysical and Biochemical Cytology 5: 11-18.

Hayes, R.A., M.R. Biehmer, L.G.J. Fokkink. 1999. A study of silica nanoparticle adsorption using optical reflectometry and streaming potential techniques. Langmuir 15: 2865-2870.

Jin, X., N.H.L. Wang, G. Tarjus, J. Talbot. 1993. Irreversible adsorption on nonuniform surfaces: the random site model. Journal of Physical Chemistry 97: 4256-4258.

Melmsten, M. 1994. Ellipsometry studies of protein layers adsorbed at hydrophobic surfaces. Journal of Colloid and Interface Science 166: 333-342.

Ramsden, J.J. 1993. Experimental methods for investigating protein adsorption kinetics at surfaces. Quarterly Reviews of Biophysics 27: 41-105.

Reisch, A., J.C. Voegel, E. Gonthier, G. Decher, B. Senger, P. Schaaf, P.J. Mésini. 2009. Polyelectrolyte multilayers capped with polyelectrolytes bearing phosphorylcholine and triethylene glycol groups: parameters influencing antifouling properties. Langmuir 25: 3610-3617.

Schaaf, P., J. Talbot. 1989. Surface exclusion effects in adsorption processes. Journal of Chemical Physics 91: 4401-4409.

Toscano, A., M.M. Santore. 2006. Fibrinogen adsorption on three silica-based surfaces: conformation and kinetics. Langmuir 22: 2588-2597.

Vasina, E.N., P. Dejardin. 2004. Adsorption of a-chymotrypsin onto mica in laminar flow conditions. Adsorption kinetic constant as a function of tris buffer concentration at pH 8.6. Langmuir 20: 8699-8706.

Wasilewska, M., Z. Adamczyk. 2011. Fibrinogen adsorption on mica studied by AFM and *in situ* streaming potential measurements. Langmuir 27: 686-696.

Wasilewska, M., Z. Adamczyk, B. Jachimska. 2009. Structure of fibrinogen in electrolyte solutions derived from dynamic light scattering (DLS) and viscosity measurements. Langmuir 25: 3698-3704.

Wertz, Ch.F., M.M. Santore. 2001. Fibrinogen adsorption on hydrophilic and hydrophobic surfaces: geometrical and energetic aspects of interfacial relaxations. Langmuir 17: 3006-3016.

Zembala, M., Z. Adamczyk. 2000. Measurements of streaming potential for mica covered by colloid particles. Langmuir 16: 1593-1601.

Zembala, M., Z. Adamczyk, P. Warszyński. 2003. Streaming potential of mica covered by latex particles. Colloids and Surfaces A 222: 329-339.

Zembala, M., P. Dejardin. 1994. Streaming potential measurements related to fibrinogen adsorption onto silica capillaries. Colloids and Surfaces B 3: 119-129.

Zembala, M., J.C. Voegel, P. Schaaf. 1998. Elution process of adsorbed fibrinogen by SDS: competition between removal and anchoring. Langmuir 14: 2167-2173.

Yoon, J.Y., H.Y. Park, J.H. Kim, W.S. Kim. 1996. Adsorption of BSA on highly carboxylated microspheres - quantitative effects of surface functional groups and interaction forces. Journal of Colloid and Interface Science 177: 613-620.